Chapter 4

PSP Corrections

4.1 Relationships Between PIR Parameters and PSP Thermal Offset

4.1.1 Theoretical Considerations

Several authors [5, 6, 13] suggest that the thermal offset in a PSP is highly correlated to the output signal of a PIR. Figure 4.1 shows a scheme of the energy exchanges inside a PSP and a PIR. The temperature gradient between the dome and the body of a PSP is responsible for the thermal offset in the instrument. This difference in temperature is produced by a infrared radiation heat exchange between the dome of the PSP and the sky. The net radiative flux between the dome and the sky (and hence the amount of thermal offset) depends on atmospheric conditions. Large offsets correspond to clear sky conditions or high-altitude clouds whereas small offsets are found under low-altitude cloud decks.

The PIR is an instrument designed to measure the upwelling or downwelling infrared radiation. The output signal of a PIR is proportional to the net IR on its detector as described in Chapter 2. The net IR signal output is composed of a downwelling component from the sky, a downwelling component from the dome and an upwelling component from the detector. The downwelling component from the sky is proportional to the brightness

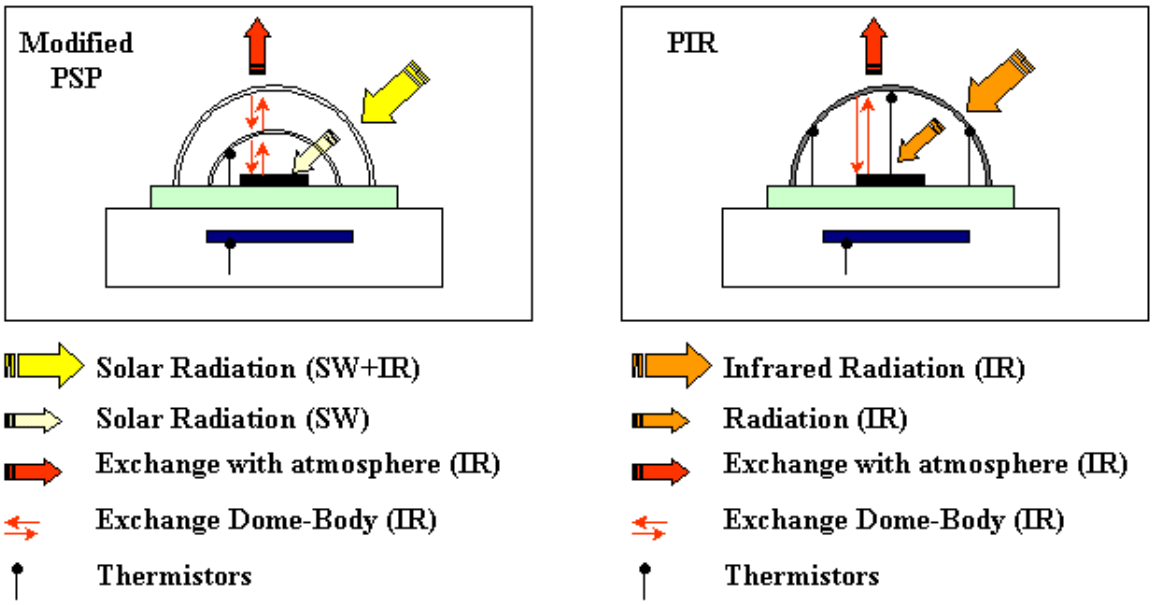

Figure 4.1: Scheme of the radiative energy balance in a modified PSP and a PIR.

temperature of the sky which depends on the fraction of cloud cover, the altitude of the cloud base, the optical depth of the cloud and the water vapor content of the atmosphere. The thermal offset of the PSP depends on the same parameters. A relationship between netIR and the thermal offset must exist since the thermal offset and the net IR measured by the PIR are both sensitive to the brightness temperature of the sky.

Figure 4.2(a) shows the output of PSP 30849 F3 and its thermal offset and Figure 4.2(b) shows the output of PIR 30355, around sunset on day 284, 2000. Before sunset the net IR signal remains fairly constant. As the sun sets a transient process starts until the the net IR signal reaches a steady state with the nighttime conditions. A similar situation happens with the offset; the daytime offset is larger than the nighttime offset due to the influence of solar irradiance in the temperature of the body. When the sun

sets the thermal offset starts a transient process that follows the one of the PIR. Figure 4.2(a) and (b) illustrate quantitatively that the thermal offsets follows the net IR signal very well, even in a strong transient process.

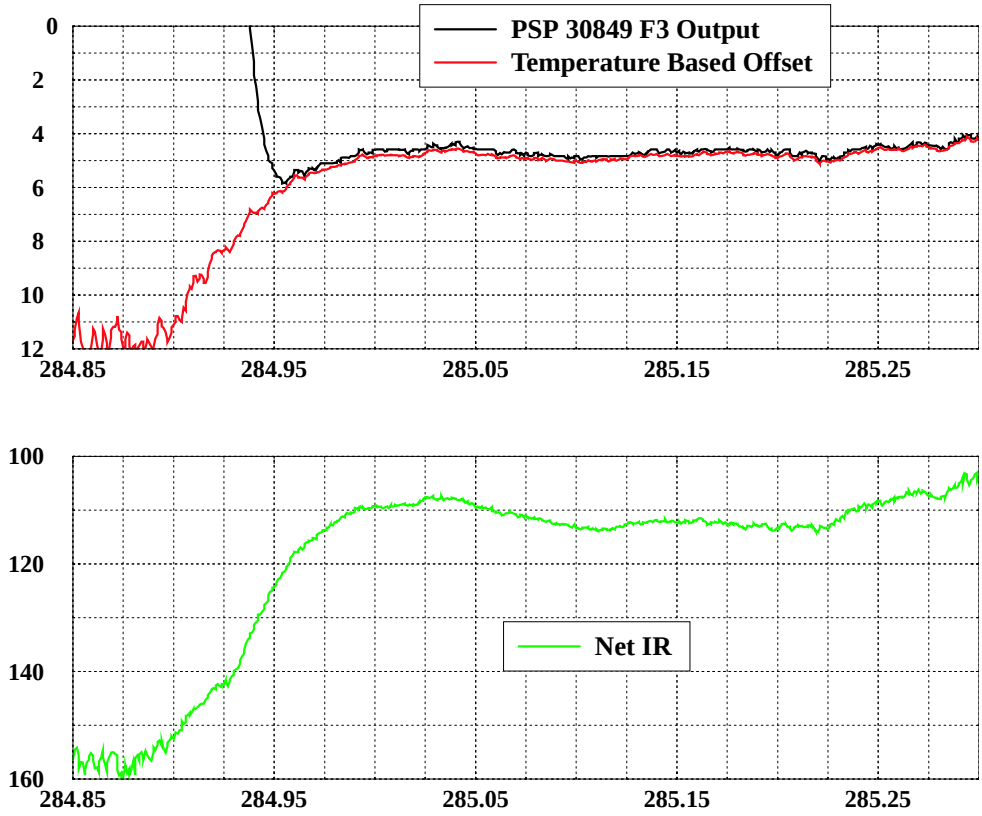

Figure 4.2: (a)Output of PSP 30849 F3 at the sunset of day 284 and night of day of the year 285 (b)netIR during the sunset of day 284 and night of day 285

4.1.2 Nighttime Correlation

To find a relationship between the net IR and the thermal offset we follow the same steps used in the characterization of the the thermal offset in Chapter 3. Firstly, a relationship must be established at night when the thermal offset is given by the PSP output. Secondly, the nighttime relationship is applied during daytime and validated.

Figure 4.3 shows two scatterplots of the output of PSP 30849F3 and PSP 31562F3 versus the net IR of PIR 30355. The PSP data are averaged for 1 Wm^{-2} interval of NetIR. The binned data are plotted in red. A linear regression of the binned data is plotted in yellow and a linear regression forced through zero of the scattered data is plotted in green. Both PSP's are operating on an Eppley tracker. The data are taken from the LaRC data

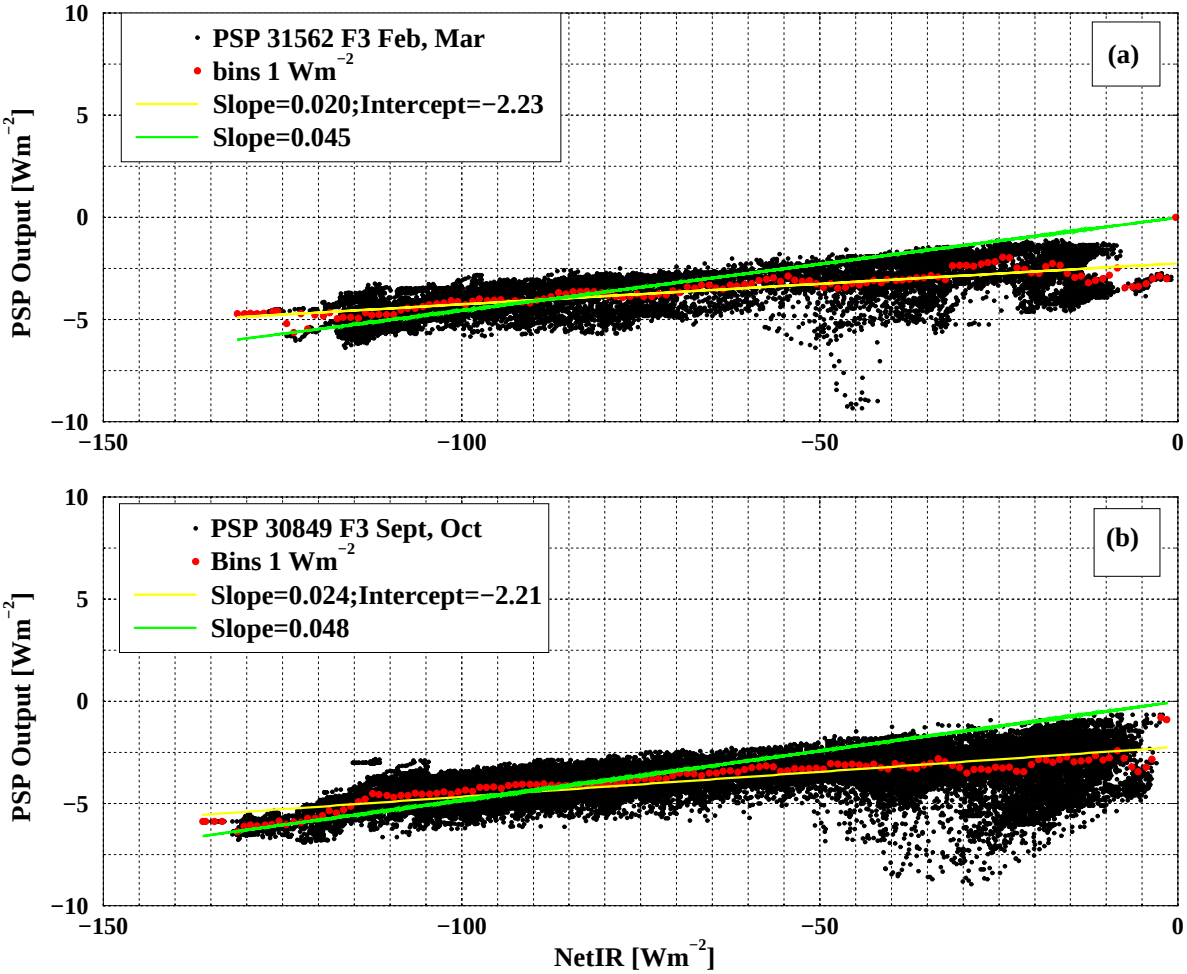

Figure 4.3: PSP output versus Net IR at night (a) PSP 31562 F3 and (b)PSP 30849 F3.

set. The PSP 30849F3 data were collected from September to December 2000 and the PSP 31562F3 data from February and March 2001.

The output of both PSP's depend linearly on the net IR. The coefficients of the linear regressions shown in Figure 4.3 are given in Table 4.1. Several authors [2] suggest that the linear regression should be forced through zero because a zero PSP signal should correspond to a PIR output of zero. The coefficients of the linear regression forced through zero, shown in Figure 4.3, is also given in Table 4.1

The coefficients are similar for both instruments. The difference between the two data sets is less than a 5 %, although the time of the year of the data is completely different. These results are also consistent with those of Haeffelin et al. [13]. The value of the coefficient of the linear regression forced through zero depends on the ventilation of the PSP, because the PSP offset depends on the ventilation.

	Linear Regression		Linear Regression Forced through Zero	
Instrument	Slope (-)	Intercept $[Wm^{-2}]$	Slope (-)	Intercept $[Wm^{-2}]$
PSP 30849 F3	0.020	-2.23	0.045	0
PSP 31562 F3	0.024	-2.21	0.045	0

Table 4.1: Coefficients of the linear regressions for PSP 30849 F3 and PSP 31562 F3 plotted in Figure 4.3.

Deviation from the linearity

Figure 4.3 shows a linear relationship between the output of the PSP at night (thermal offset) and the net IR. When the net IR output is larger than -50 W/m^2 the sky is typically overcast; in some cases the PSP output fall well below the regression line. This is a situation in which rain or snow can be present. Radiation heat exchange with the atmosphere drives the temperature of the dome, however if the dome is covered with water droplets, as is the case under rainy conditions, the evaporation of the water droplets will produce additional dome cooling. The evaporation depends on the air flow. Therefore under rainy conditions the relationship between the thermal offset and the net IR changes.

Variation of the slope with ventilation

Figure 4.3 shows the nighttime relationship between the PSP output and the net IR for two different PSP's. Both PSP's are working with the same ventilation systems and the regression coefficients for both instruments are similar. However a change in ventilation will modify the slope as is shown in Figure 4.4.

Figure 4.4 (a) shows the output of PSP 31562 F3 versus the net IR when the PSP and the PIR are mounted on an Eppley tracker and operate with the standard Eppley fan in February and March 2001. Figure 4.4(b) shows the output of PSP 31562 F3 versus the net IR when the PSP is operating with two different types of fans on fix stands whereas the PIR is still mounted on an Eppley tracker. Data from PSP on fan I and fan II are plotted in black and red, respectively. PSP 31562 F3 was operated on fan I in

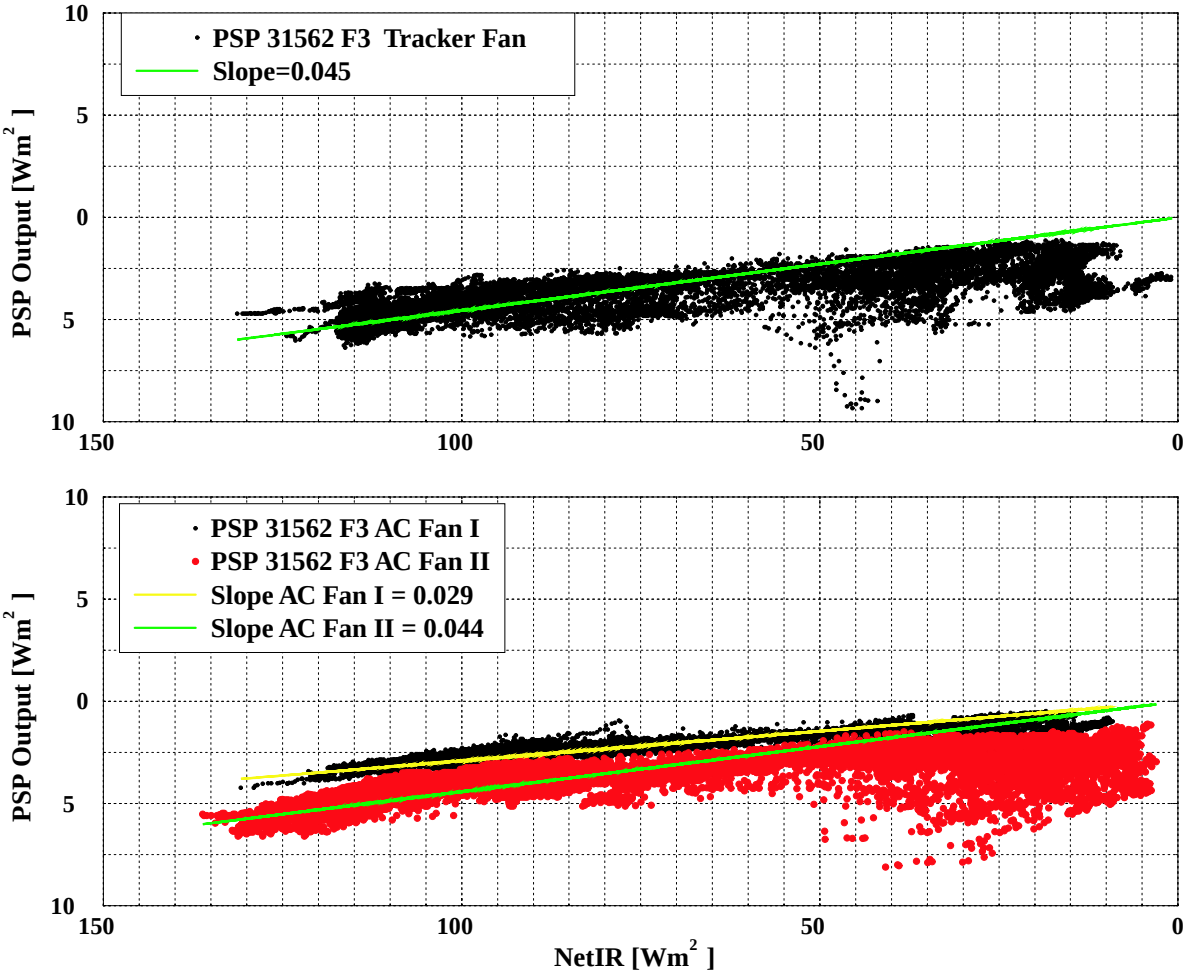

Figure 4.4: Net IR versus PSP output at night for (a) 31562 F3 mounted on an Eppley tracker and (b)PSP 31562 F3 mounted on two different fix stands.

September and October 2000 and on fan II in November 2000. Table 4.2 shows the slopes of the regression of the scatterplots without forcing the regression through zero (columns 2 and 3) and forcing the regression through zero (column 3). The slope of the regression not forced through zero remains constant in all the cases, however the intercept varies depending on the efficiency of the ventilation. The intercepts are -0.81 W m^{-2} and -2.21 W m^{-2} for the fix stand fan I and the tracker fan, respectively. These results show that the better the ventilation is the smaller the offset.

When the regression is forced through zero the slope of the regression varies with ventilation. The smallest regression slope correspond to the most efficient ventilator. Note that a change in PIR ventilator will modify the slopes as well.

Instrument	Slope (-)	Intercept $[Wm^{-2}]$	Slope (-)
Tracker Fan	0.020	-2.21	0.045
Fix Stand Fan I	0.019	-0.81	0.029
Fix Stand Fan II	0.019	-2.19	0.044

Table 4.2: Variation of the coefficients for the linear relationship PSP output at night versus net IR depending on ventilation conditions

4.1.3 Daytime Correlation

A linear relationship between the thermal offset (PSP output) and the net IR has been established at night. Now, the challenge is to find if this relationship can be applied to predict daytime offsets.

Figure 4.5 shows the scatterplots of the temperature-based offset estimate versus the net IR for PSP 31562 F3 and PSP 30849 F3. Both instruments are operating on the solar tracker. The thermal offset depends on the net IR as has been observed at night. A linear regression, shown in red, is fitted through the data. A regression, forced through zero, is plotted in yellow.

	Slope Forced Zero		Not forced through zero			
	Night (-)	day (-)	Slope day (-)	Inter day $[Wm^{-2}]$	Slope night (-)	Inter. night $[Wm^{-2}]$
PSP 31562 F3	0.045	0.068	0.049	-2.6	0.020	-2.23
PSP 30849 F3	0.048	0.064	0.048	-1.97	0.024	-2.21

Table 4.3: Comparison of the coefficients for the net IR regression during daytime and nighttime

Table 4.3 shows the data of Figures 4.5 and 4.3. If the regression is forced through zero the nighttime slope and the daytime slope differ substantially, however the nighttime slope forced through zero and the daytime slope not forced through zero are similar. This

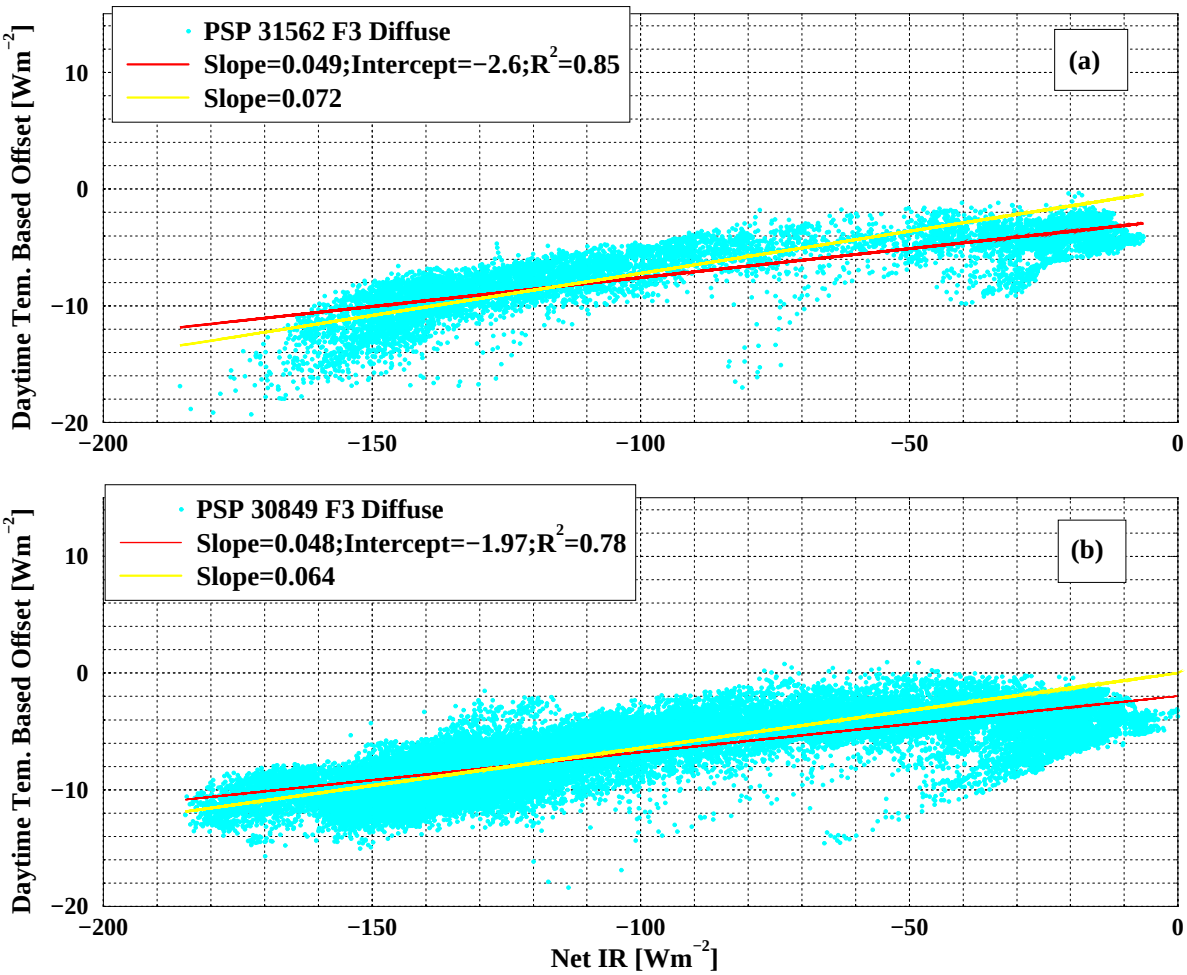

Figure 4.5: Net IR versus PSP temperature-based offset for (a) PSP 31562 F3 and (b)PSP 30849 F3. Both instrument are mounted on an Eppley solar tracker.

behavior is due to the fact that during daytime the offsets are much larger that during nighttime. The net IR measured by the PIR decreases during daytime but not at the same rate as the PSP offset. For example during nighttime the offset of PSP 30849 F3 ranges from 0 Wm^{-2} to -7 Wm^{-2} and the net IR ranges from 0 Wm^{-2} to values close to -135 Wm^{-2}. However during daytime for the same instrument the offset ranges from 0 to -15 Wm^{-2}, twice the nighttime offset. The values of the net IR do not double but range from 0 to -190 Wm^{-2}.

4.1.4 Data Correction

Figure 4.6 and 4.7 show the frequency of occurrence of the PSP offset (blue) and the PSP offset corrected with the net IR-based offset estimate (red). Data from PSP 30849 F3 and PSP 31562 F3 are shown in Figure 4.6 and Figure 4.7, respectively. The PSP offset is derived from the PSP temperature measurements. Both graphs show a bi-modal distribution of the offset associated with the population of clear skies and overcast skies.

	PSP Offset $[Wm^{-2}]$		Offset Corrected using Net IR data $[Wm^{-2}]$	
	Mean	Std. Dev.	Mean	Std. Dev.
PSP 30849 F3	-6.8	2.8	-2.1	1.7
PSP 31562 F3	-6.3	3.1	-3.0	1.6

Table 4.4: Net IR correction for PSP 31562 F3 and PSP 30849 F3

Table 4.4 shows the mean and standard deviation of the temperature-estimated offset and the remaining offset after correction. The correction reduces the offset by about 70 % for PSP 30849 F3 and 50% for PSP 31562 F3. The standard deviation around the mean is also reduced 51 % for PSP 31562 F3 and 40 % for PSP 30849 F3. The standard deviation is due to the noise of the measurement that cannot be reduced with the correction.

4.2 Relationship between the Cloud Cover Fraction and the PSP Thermal Offset

4.2.1 Theoretical Considerations

The thermal offset of a PSP is due to a radiation heat exchange between the dome of the instrument and the sky. The amount of heat exchanged and hence the value of the thermal offset depends on the brightness temperature of the sky, which is the temperature of the sky if it were a blackbody. The colder the sky is the larger the offset. The brightness

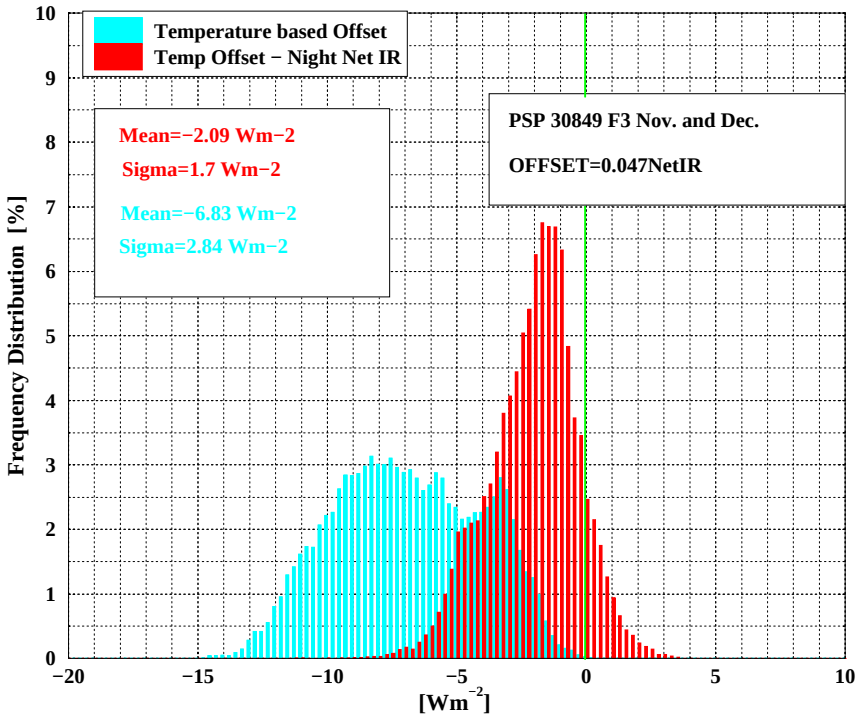

Figure 4.6: Correction of the daytime offset of PSP 30849 F3 using the relationship between PSP offset and net IR.

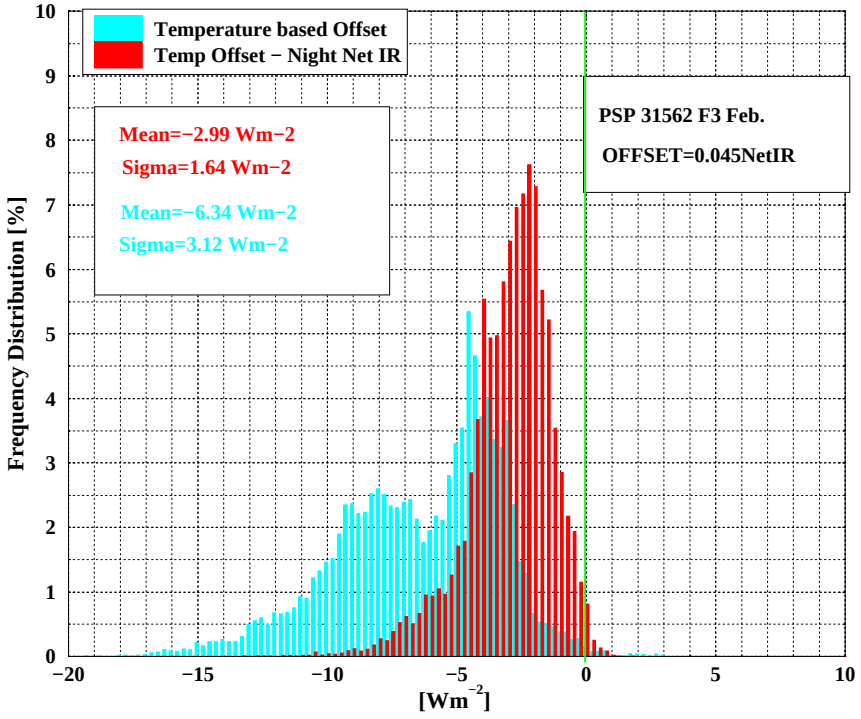

Figure 4.7: Correction of the daytime offset of PSP 31562 F3 using the relationship between PSP offset and net IR.

temperature of the sky depends on several factors such as the fraction of cloud cover, the altitude of the cloud base, the optical depth of the cloud, and the water vapor content of the atmosphere. Therefore the thermal offset should also depend on the amount and distribution of clouds.

The cloud cover fraction is the percentage of the sky that is covered by clouds. It goes from completely clear sky 0 % to overcast 100 %. There are several methods to determine the cloud cover, one of them uses measurements of the global and diffuse surface irradiance [17, 18, 19, 20], another is based on the downwelling infrared irradiance measured by PIR [21]. If a relationship between the cloud fraction and the thermal offset exits the thermal offset could be retrieved in non-modified PSP's using only data coming from the PSP's. Although typically PIR's operate in conjunction with PSP's many sites do not provide any PIR data. This relationship would help to correct historical data from isolated PSP's.

4.2.2 The Long-Ackermann Algorithm

The cloud amount and its effects on global radiative energy balance is one of the main uncertainties in climate [17]. Satellites are used to provide global cloud coverage, however satellite data must be validated. The validation of satellite global cloud coverage was done using observer's reports. Long and Ackerman [17, 18, 19, 20] created an algorithm based on the ratio between clear-sky diffuse irradiance and the irradiance under other conditions to determine the cloud clover. This algorithm has the advantage that it eliminates the sometimes subjective reports and temporal and spatial mis-matches of the observers. It also has the advantage of only using data coming from pyranometers, which are instruments widely spread out over the whole planet.

The algorithm is first based in the detection of clear-sky periods using the fact that the ratio of the solar diffuse irradiance to the total downwelling solar irradiance is minimum under clear sky conditions [19]. Once the periods of clear-sky conditions are determined "an empirical fitting algorithm is applied that uses a minimum absolute deviation fitting technique to estimate both the clear sky total SW irradiance and the ratio of diffuse to total SW irradiance as a function of the zenith angle" [18]. Once this is known the cloud cover can be retrieved using the diffuse-to-total ratio.

4.2.3 Daytime Correlation

Figure 4.8 shows a scatterplot of the cloud cover fraction found using the Long/Ackerman algorithm versus the temperature-based offset of PSP 30849 F3 in September and October 2000. A linear regression is fitted through the data. The data are binned into 5 % cloud

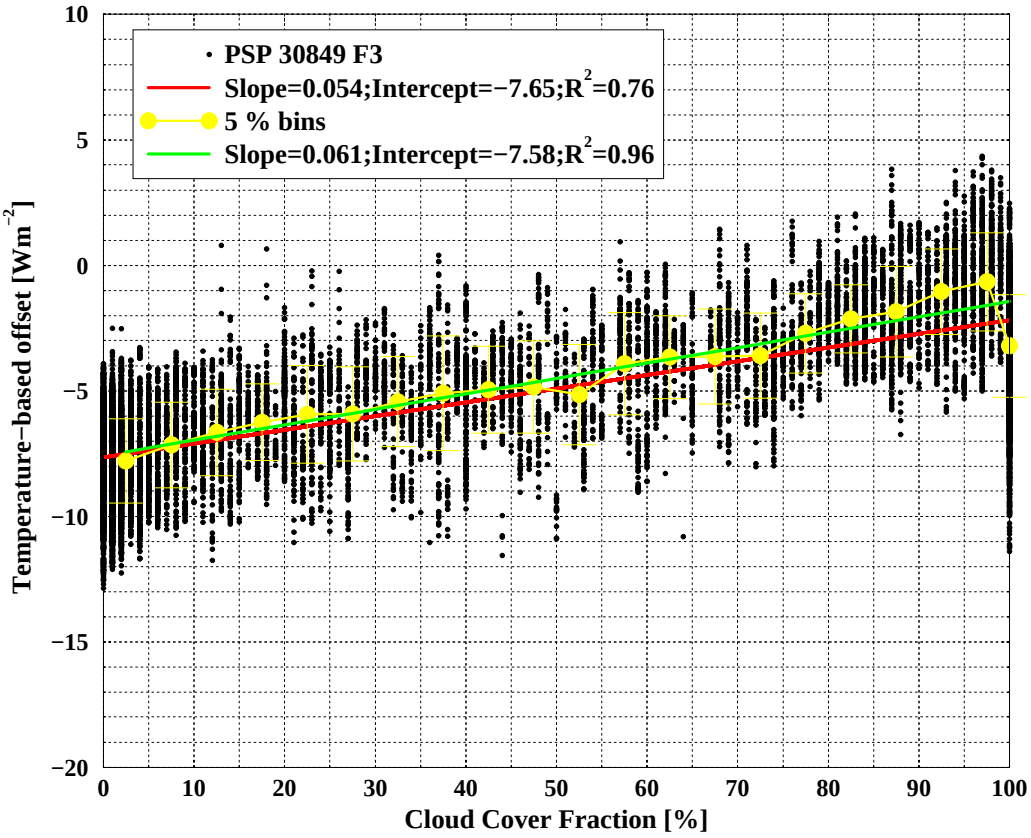

Figure 4.8: Relationship between cloud cover fraction and temperature-based offset estimate from PSP 30849 F3 data collected in September and October 2000

cover intervals in order to reduce the noise. A linear regression, shown in green, is fitted through the binned data. Figure 4.8 shows a strong linear dependence of the temperature-based offset estimate with the cloud cover fraction that proves the hypothesis defined in the previous section. However there are several concerns. The first one is the noise; the dispersion of the points in the scatterplot diagram is significant. The R^2 of the linear regression on these points is only 76 %, which means that only 76 % of the variability in the data is explained by the linear regression. This is due to the fact that the cloud cover fraction does not distinguish between high level and low-level clouds and the offset produced by a low-level (warm) cloud is smaller than the one produced by high-level (cold) clouds. It is apparent for overcast conditions that the type of cloud can have a significant effect on the offset. Note that the offset ranges from 1 Wm^{-2} to -11 Wm^{-2} for 100% cloud cover fraction. Precipitation is another factor that is not taken into account when using the cloud cover fraction, however, the binned data are very stable from 0% to 90 % cloud cover. The R^2 of the linear regression fitted through the binned data is 0.96. Hence, this relationship can be considered a fairly good first approximation because although there are some uncertainties exist under overcast conditions the relationship works fine under clearer skies.

Instrument	Slope	0% Intercept [Wm^{-2}]	100% Intercept [Wm^{-2}]
PSP 30849 F3 Sep. 00	0.052	-9.0	-3.8
PSP 30849 F3 Oct. 00	0.048	-9.8	-5.0
PSP 30849 F3 Nov. 00	0.056	-9.3	-3.7
PSP 30849 F3 Dec. 00	0.054	-10.2	-4.8
PSP 31562 F3 Feb. 00	0.049	-10.6	-5.7
PSP 30849 F3 Sep./Oct. 00	0.052	-10.0	-4.4
PSP 30849 F3 Nov./Dec. 00	0.056	-9.5	-4.3
PSP 30849 F3 Sept/Dec 00	0.054	-9.6	-4.2

Table 4.5: Parameters of the regression used to estimate the PSP offset from cloud cover data

Table 4.5 shows the values of the slope of the cloud cover regression for PSP 30849 F3 and PSP 31562 F3 month by month and for the whole data set. The slope remains similar in all cases. However to retrieve the thermal offset using the cloud cover relationship it is necessary to determine an intercept point (assuming the slope is fairly constant for all instruments), defined as either the mean offset under clear sky or under overcast conditions.

4.2.4 Data Correction

Figure 4.9 and Figure 6.2 show the frequency of occurrence of the PSP offset (blue) and the PSP offset corrected with the cloud cover offset estimate (red). Data from PSP 30849 F3 and PSP 31562 F3 are shown in Figure 4.9 and Figure 6.2, respectively. The PSP offset is derived from the PSP temperature measurements. Both graphs show a bi-modal distribution of the offset associated with the clear-sky and overcast populations. The coefficients of the cloud cover relationships for PSP 30849 F3 are derived using data from September and October, then the relationship is applied to data of November and December. The coefficients of the cloud cover relationships for PSP 31562 F3 are derived

	PSP Offset [Wm^{-2}]		Offset Corrected using cloud cover data [Wm^{-2}]	
	Mean	Std. Dev.	Mean	Std. Dev.
PSP 30849 F3	-6.8	2.8	0.1	1.8
PSP 31562 F3	-6.3	3.1	0.5	1.9

Table 4.6: Cloud Fraction Correction for PSP 31562 F3 and PSP 30849 F3

using data from February and March, then the relationship is applied to data of February and March.

Table 4.6 shows the values of the daytime temperature based offset and the offset remaining after correction. The values of the mean error after correction are smaller than using the the net IR correction. The standard deviation for both PSP's are similar to that from the net IR correlation. The correlation seems to work fine, however it presents several uncertainties, the main one being the starting point needed to correct historical data.

4.3 Conclusions

The thermal offset in PSP's is related to the radiation heat exchange between dome and sky. Therefore the temperature at which the sky is emitting energy is an important factor to take into account when deriving the offset. The output signal from a PIR also depends on the temperature of the sky; effective the fraction of cloud cover is also related to the overall sky temperature is related to the fraction of cloud cover. Two methods are proposed to retrieve thermal offsets in non-modified PSP's.

$$Offset = A(netIR) \tag{4.1}$$

$$Offset = B(CF) + C \tag{4.2}$$

where A is a coefficient determined from a regression forced through zero of PSP output versus net IR at night, CF is the cloud cover fraction extracted from the Long/Ackerman algorithm and B and C are coefficients derived from a regression between PSP offset and CF.

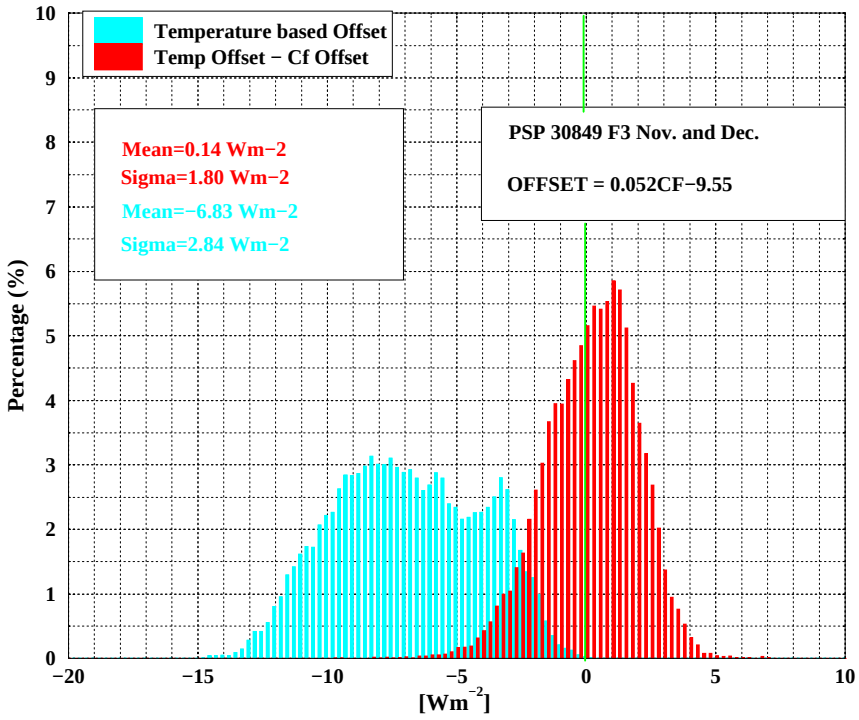

Figure 4.9: Correction of the daytime offset of PSP 30849 F3 using cloud fraction relationship

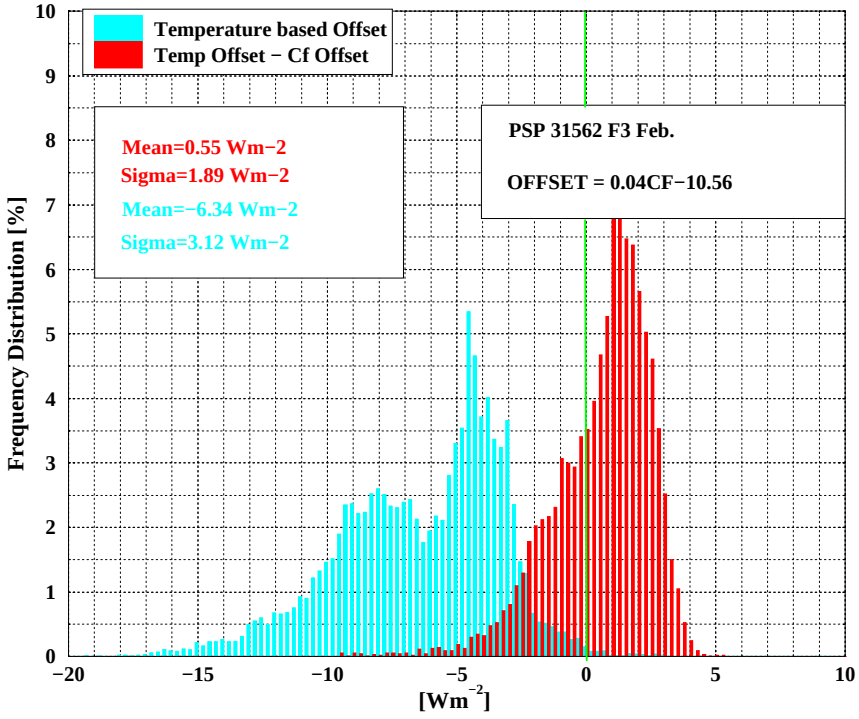

Figure 4.10: Correction of the daytime offset of PSP 31562 F3 using cloud fraction relationship

The net IR correlation has the advantage that it can be easily used in places where the net IR and the PSP output is recorded, however it seems to undercorrect the offset. The Cloud Cover Fraction correlation provides a good correlation to the data on average however the uncertainty of the types of clouds and the unknown coefficients B, C for non-modified PSP's make it difficult to be apply to recover historical data.